

# D' domain region Arg782-Cys799 of von Willebrand factor contributes to factor VIII binding

Małgorzata A. Przeradzka,<sup>1</sup> Josse van Galen,<sup>1</sup> Eduard H.T.M. Ebberink,<sup>1</sup>  
Arie J. Hoogendijk,<sup>1</sup> Carmen van der Zwaan,<sup>1</sup> Koen Mertens,<sup>1</sup>  
Maartje van den Biggelaar<sup>1</sup> and Alexander B. Meijer<sup>1,2</sup>

<sup>1</sup>Department of Molecular and Cellular Hemostasis, Sanquin Research, Amsterdam and

<sup>2</sup>Department of Biomolecular Mass Spectrometry and Proteomics, Utrecht Institute for Pharmaceutical Sciences, Utrecht University, Utrecht, the Netherlands



Haematologica 2020  
Volume 105(6):1695-1703

## ABSTRACT

In the complex with von Willebrand factor (VWF) factor VIII (FVIII) is protected from rapid clearance from circulation. Although it has been established that the FVIII binding site resides in the N-terminal D'-D3 domains of VWF, detailed information about the amino acid regions that contribute to FVIII binding is still lacking. In the present study, hydrogen-deuterium exchange mass spectrometry was employed to gain insight into the FVIII binding region on VWF. To this end, time-dependent deuterium incorporation was assessed in D'-D3 and the FVIII-D'-D3 complex. Data showed reduced deuterium incorporation in the D' region Arg782-Cys799 in the FVIII-D'-D3 complex compared to D'-D3. This implies that this region interacts with FVIII. Site-directed mutagenesis of the six charged amino acids in Arg782-Cys799 into alanine residues followed by surface plasmon resonance analysis and solid phase binding studies revealed that replacement of Asp796 affected FVIII binding. A marked decrease in FVIII binding was observed for the D'-D3 Glu787Ala variant. The same was observed for D'-D3 variants in which Asp796 and Glu787 were replaced by Asn796 and Gln787. Site-directed mutagenesis of Leu786, which together with Glu787 and Cys789 forms a short helical region in the crystal structure of D'-D3, also had a marked impact on FVIII binding. The combined results show that the amino acid region Arg782-Cys799 is part of a FVIII binding surface. Our study provides new insight into FVIII-VWF complex formation and defects therein that may be associated with bleeding caused by markedly reduced levels of FVIII.

## Introduction

The multimeric glycoprotein von Willebrand factor (VWF) acts as a carrier protein for coagulation factor VIII (FVIII) in the circulation.<sup>1</sup> In the complex with VWF, FVIII is protected from rapid clearance from plasma.<sup>2,3</sup> Multiple amino acid substitutions have been identified in VWF that impair FVIII-VWF complex formation. The associated reduced plasma levels of FVIII can result in the bleeding disorder referred to as von Willebrand disease type 2 Normandy (VWD type 2N).<sup>4</sup> Most of the aberrant mutations in VWF involve substitutions of amino acid residues that have been proposed to affect the structural integrity of VWF.<sup>5,6</sup> These substitutions provide therefore only limited information about the identity of the FVIII binding site on VWF.

Distinct protein domains can be identified in the primary amino acid sequence of VWF. These domains are arranged in the order: D'-D3-A1-A2-A3-D4-B-C1-C2-C2-CK.<sup>7</sup> Zhou *et al.* have refined the domain organization within VWF. For D'-D3, they proposed that these domains can be further divided into TIL'-E'-VWD3-C8\_3-TIL3-E3 subdomains.<sup>8</sup> In plasma, VWF circulates as an ensemble of multimeric proteins of varying size. In these multimers, the VWF monomers are head-to-head and tail-to-tail connected *via* disulphide bridges between two D3 domains and two CK domains.<sup>9</sup> FVIII also comprises multiple domains that together constitute a light chain of the domains A3-C1-C2 and a heavy chain comprising the domains A1-A2-

## Correspondence:

ALEXANDER B. MEIJER  
s.meijer@sanquin.nl

Received: March 20, 2019.

Accepted: September 25, 2019.

Pre-published: September 26, 2019.

doi:10.3324/haematol.2019.221994

Check the online version for the most updated information on this article, online supplements, and information on authorship & disclosures: [www.haematologica.org/content/106/6/1695](http://www.haematologica.org/content/106/6/1695)

©2020 Ferrata Storti Foundation

Material published in *Haematologica* is covered by copyright. All rights are reserved to the Ferrata Storti Foundation. Use of published material is allowed under the following terms and conditions:

<https://creativecommons.org/licenses/by-nc/4.0/legalcode>.  
Copies of published material are allowed for personal or internal use. Sharing published material for non-commercial purposes is subject to the following conditions:  
<https://creativecommons.org/licenses/by-nc/4.0/legalcode>, sect. 3. Reproducing and sharing published material for commercial purposes is not allowed without permission in writing from the publisher.



B.<sup>10</sup> Because of limited proteolysis of the B domain, FVIII is heterogeneous in size with molecular weights ranging from 160 kDa to 330 kDa.<sup>11,12</sup>

For effective binding to FVIII, VWF requires the presence of a short acidic amino acid region at the start of the FVIII A3 domain. This region, which includes sulphated tyrosine residues, is referred to as the  $\alpha 3$  region.<sup>13,14</sup> Next to this VWF binding region, hydrogen-deuterium exchange mass spectrometry (HDX-MS) and previous site-directed mutagenesis studies have identified binding sites for VWF in the C1 and C2 domain of FVIII as well.<sup>15-19</sup> During activation of FVIII, the  $\alpha 3$  region is removed from FVIII leading to the dissociation of the FVIII-VWF complex. Additional cleavages by thrombin generates activated FVIII that can perform its role in the coagulation cascade as a cofactor for activated factor IX ultimately leading to fibrin formation.<sup>20</sup>

It has previously been established that the N-terminal D'-D3 domains of VWF comprise the binding site for FVIII. In 1987, limited proteolysis studies of VWF revealed that a VWF fragment comprising the residues 764-1036 harbors the interaction site for FVIII.<sup>21</sup> Based on cryoelectron microscopy (cryo-EM) structures of FVIII in complex with D'-D3, it has later been shown that the main interactive region for FVIII resides in the D' domain.<sup>19</sup> Recently, we have found that the presence of the VWD3 subdomain of the D3 domain is required to optimally support the interaction between D' and FVIII.<sup>22</sup> Using a primary amine-directed chemical foot printing approach combined with mass spectrometry analysis, we have further demonstrated that Lys773 contributes to FVIII binding.<sup>23</sup> In the present study, we have employed HDX-MS combined with site-directed mutagenesis and protein binding studies to further explore the FVIII binding regions on VWF. The combined results show that the D' domain region Arg782-Cys799 is part of the FVIII binding interface.

## Methods

### Materials

Tris-HCl was from Invitrogen (Breda, the Netherlands), NaCl was obtained from Fagron (Rotterdam, the Netherlands) and HEPES was from Serva (Heidelberg, Germany), FreeStyle 293 expression medium was obtained from Gibco (Thermo Fisher Scientific). Tween-20 and D<sub>2</sub>O was from Sigma-Aldrich (St Louis, MO, USA). Human serum albumin (HSA) was obtained from the Division of Products at Sanquin (Amsterdam, the Netherlands). All other chemicals were from Merck (Darmstadt, Germany), unless indicated otherwise.

### Proteins

Antibody CLB-EL14 (EL14), CLB-Rag20, CLB-CAg12 (CAg 12) and HPC4 have been described before.<sup>22,24,25</sup> D'-D3 fragment, FVIII lacking the B domain residues 746-1639 (referred to as FVIII throughout this paper) and VWF were obtained essentially as described before.<sup>26-28</sup> Purified proteins were dialyzed against a buffer with 50 mM HEPES (pH 7.4), 150 mM NaCl, 10 mM CaCl<sub>2</sub>, 50% (v/v) glycerol and stored at -20°C. Site-directed mutagenesis of the D'-D3 fragment was employed using Quik Change (Agilent Technologies) according to the manufacturer's instructions.

### HDX-MS

D'-D3 was pre-incubated in presence or absence of FVIII in 1:1 molar ratio for 5 min at 4°C. Samples were subsequently diluted

ten times in deuterated binding buffer (98% D<sub>2</sub>O) or standard binding buffer and incubated for 10 sec, 100 sec or 1,000 sec at 24°C. A detailed description is available in the *Online Supplementary Materials and Methods*.

### Solid-phase competition assays

Recombinant VWF (1 µg/mL) was immobilized overnight at 4°C in a buffer containing 50mM NaHCO<sub>3</sub> pH 9.8 in a 96-wells microtiter plate (Nunc Maxisorp). Increasing concentrations (0.3-900 nM) of D'-D3 and variants with single mutations were pre-incubated with 0.3 nM FVIII in a buffer containing 50 mM Tris, 150 mM NaCl, 2% human serum albumin, 0.1% Tween 20, pH 7.4 for 30 min at 37°C. These mixtures were transferred to the VWF coated plate and incubated for 2 hours at 37°C. Then, the plate was washed three times with 50 mM Tris (pH 7.4), 150 mM NaCl, 5mM CaCl<sub>2</sub>, 0.1% Tween 20 after which FVIII bound to VWF was detected with an HRP-labeled monoclonal antibody (CAg 12).<sup>26</sup>

### Surface plasmon resonance analysis

Surface plasmon resonance (SPR) analysis was carried out using a Biacore T-200 biosensor system (GE Healthcare) as previously described.<sup>22</sup> A monoclonal antibody to FVIII (EL14) was coupled to a CM5 sensor chip (GE Healthcare) to 5,000 response units (RU) density using the amino coupling activation method according to manufacturer's suggestions (GE Healthcare). Subsequently, 3,000 RU of FVIII were immobilized to the chip *via* EL14 antibody. Next, increasing concentrations of D'-D3 fragments were passed over the chip at a flow rate of 30 µL/min in a buffer containing 20 mM HEPES (pH 7.4), 150 mM NaCl, 5 mM CaCl<sub>2</sub> and 0.05% Tween 20 at 25°C. An empty channel was utilized to correct for non-specific binding to the dextran matrix.

## Results

### HDX-MS on the isolated D'-D3 fragment of VWF

To facilitate identification of the FVIII binding residues within the D' domain (TIL'-E' subdomains), we made use of the D'-D3 monomer in which the cysteine residues involved in dimerization of the D3 domains (VWD3-C8\_3-TIL3-E3 subdomains) were replaced by serine residues.<sup>29</sup> The D'-D3 fragment was transferred from H<sub>2</sub>O to D<sub>2</sub>O-containing buffer to assess time-dependent deuterium incorporation into the protein backbone. 178 peptides were identified covering 92% of the D'-D3 sequence (Figure 1A and *Online Supplementary Table S1*). For each peptide, we plotted the percentage of deuterium incorporation of the identified peptides at three different time points (Figure 1B). The overall result showed that almost all peptides from the N-terminal TIL' subdomain of D'-D3 exhibit limited to no change in deuterium incorporation at these time points. Only the peptide that includes the N-terminus of the TIL' subdomain showed increased deuterium incorporation. Apart from several peptides in the C8\_3 subdomain of the D3 domain, most of the peptides in the other subdomains showed incorporation of deuterium in time. Peptides with the most marked change in deuterium incorporation correspond to unstructured regions in the recently published crystal structure of D'-D3.<sup>30</sup> This finding confirms that amino acid backbone hydrogens in unstructured regions exhibit an enhanced rate of hydrogen-deuterium exchange compared to structured regions. It further implies that these regions are unstructured in solution as can be predicted by the crystal structure.

### D' region Arg782-Cys799 shows reduced deuterium incorporation in the presence of FVIII. HDX-MS was employed on the FVIII-D'-D3 complex

The complex was transferred to D<sub>2</sub>O-containing buffer and the incorporation of deuterium was assessed at three

different time points. The obtained results were compared to the time-dependent deuterium incorporation in D'-D3 in the absence of FVIII. Most peptides originating from the FVIII-D'-D3 complex did not show a change in deuterium uptake compared to isolated D'-D3 (Figure 2 and *Online*

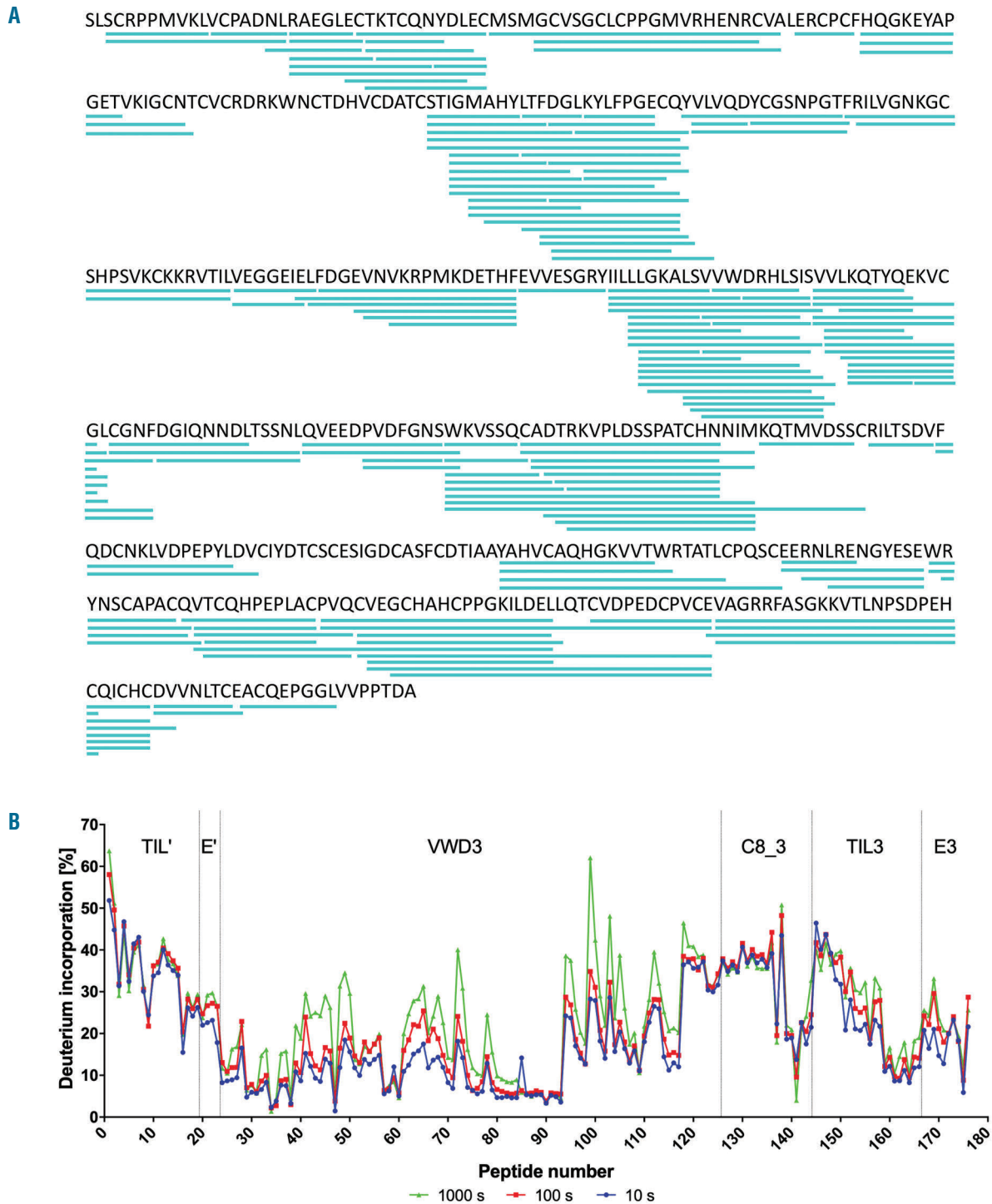


**Figure 1. Hydrogen-deuterium exchange mass spectrometry analysis of the D'-D3 fragment.** D'-D3 was incubated for 10 sec, 100 sec and 1000 sec in a deuterium buffer consisting of 20 mM HEPES (pH 7.4), 150 mM NaCl and 5 mM CaCl<sub>2</sub>. D'-D3 was processed for hydrogen-deuterium exchange mass spectrometry (HDX-MS) analysis as described in the methods. (A) Shows the identified peptides as blue lines underneath the primary sequence of D'-D3. (B) Shows the percentage of deuterium incorporation for the individual identified peptides for the different incubation times with deuterium buffer. The sequence of the peptide's numbers, shown on the x-axis, is displayed in the *Online Supplementary Table S1*.



Supplementary Figure S1). Several overlapping peptides in the TIL' subdomain of D', however, did show a reduced deuterium incorporation in the complex. The peptide region that is shared by the overlapping peptides includes the amino acids Arg782-Cys799 (Figure 2B-C). The HDX-MS results suggest that the local hydrogen bonding network is altered in this VWF region upon FVIII binding implying that this region contributes to FVIII binding.

### SPR analysis reveals that charged residues in D' region Arg782-Cys799 contribute to FVIII binding

Site-directed mutagenesis of the D'-D3 fragment was employed to verify the contribution of the region Arg782-Cys799 to FVIII binding. As electrostatic interactions have been proposed to mediate FVIII-VWF complex assembly,<sup>31,32</sup> the charged amino acids in this region were replaced by alanine residues resulting in six new D'-D3 variants *i.e.* Arg782Ala, Glu784Ala, Glu787Ala, Lys790Ala, Asp796Ala and Glu798Ala. SPR analysis was performed to assess their FVIII binding efficiency. To this end, increasing concentrations of the D'-D3 variants were passed over FVIII that was immobilized *via* antibody EL14 to the surface of a CM5 sensor chip (Figure 3A-G). The Arg782Ala, Glu784Ala and Glu798Ala variants revealed association and dissociation binding responses that closely resembled those of the wild-type (WT) D'-D3. The Lys790Ala and Asp796Ala variants showed decreased binding responses compared to WT D'-D3. Almost no

binding was observed for the Glu787Ala variant. The association and dissociation responses revealed complex binding kinetics comprising at least two components. To estimate the binding affinities, we plotted the maximum binding response as a function of the D'-D3 variant concentration (Figure 3H). The concentration at which the half-maximum binding response is reached, represents an estimation of the average binding affinities ( $\langle K_D \rangle$ ) of the involved components. Compared to the  $\langle K_D \rangle$  obtained for the WT D'-D3 (~50 nM), results showed a more than four-fold increase in  $\langle K_D \rangle$  for D'-D3 Asp796Ala (~190 nM) and a five-fold increase for D'-D3 Lys790Ala (~240 nM). These findings together show that charged amino acid residues in the region Arg782-Cys799 contribute to FVIII binding. A glutamic acid at position 787 appears most critical for effective interaction between FVIII and D'-D3.

A solid phase competition assay reveals that charged residues contribute to FVIII binding. The efficiency by which the D'-D3 variants were able to compete with VWF for FVIII binding was assessed using a competitive binding assay as also employed in previous studies.<sup>22,23</sup> FVIII was incubated with immobilized VWF in the presence of increasing concentrations of the D'-D3 variants. Residual FVIII binding to immobilized VWF was assessed using an antibody against FVIII that does not interfere with the complex formation between FVIII and VWF (Figure 4). Results showed that about 50 nM of WT D'-D3 was

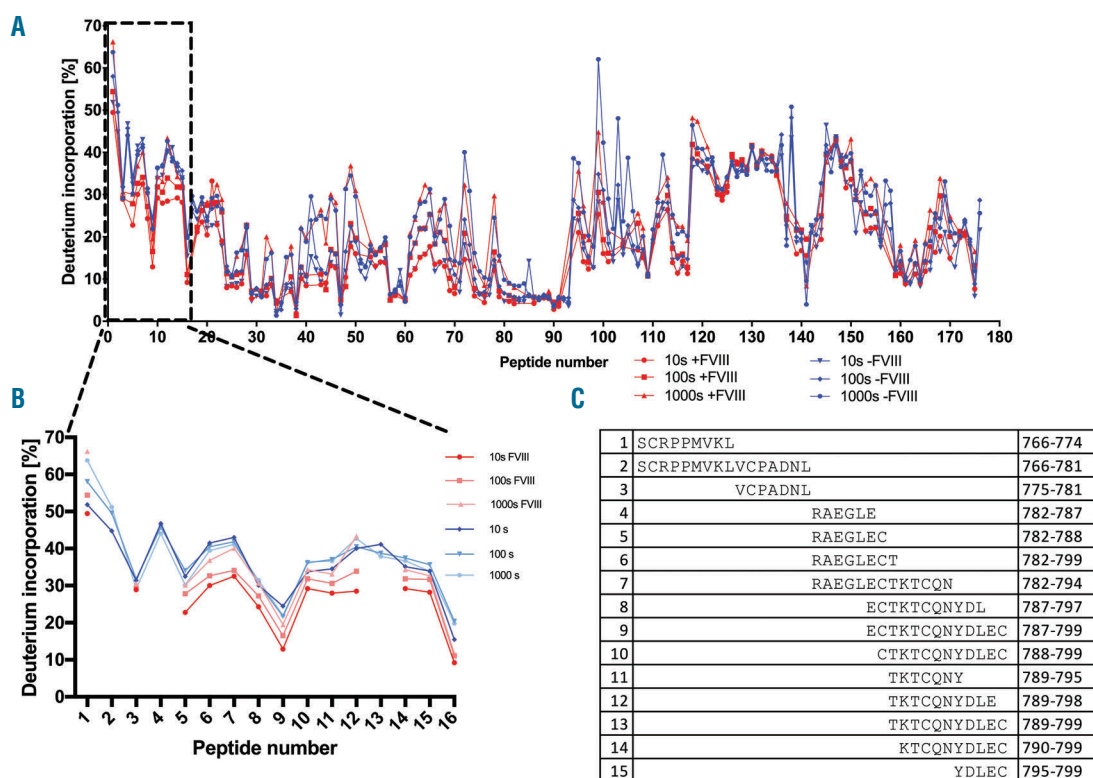


**Figure 2. Hydrogen-deuterium exchange mass spectrometry analysis of the FVIII-D3 complex.** The D'-D3 was incubated for 10 sec, 100 sec and 1000 sec in a deuterium buffer consisting of 20 mM HEPES (pH 7.4), 150 mM NaCl and 5 mM CaCl<sub>2</sub> in the presence and absence of coagulation factor VIII (FVIII). The proteins were processed for hydrogen-deuterium exchange mass spectrometry (HDX-MS) analysis as described in the methods. (A) Shows the percentage of deuterium incorporation of the identified peptides of the D'-D3 at the indicated incubation times in deuterium buffer in the presence and absence of FVIII. The sequence of the peptide numbers, shown on the x-axis, is displayed in the *Online Supplementary Table S1*. (B) Shows the percentage of time-dependent deuterium incorporation for the 15 identified peptides that cover part of the TIL' subdomain of D'. The sequence of the peptide numbers, shown on the x-axis, is displayed in (C).

required to reduce FVIII binding to immobilized VWF by 50%. For the Arg782Ala, Glu784Ala, and Glu798Ala variants of D'-D3 about 100 nM was required to reach the same effect. A markedly reduced competition efficiency was observed for the Asp796Ala variant as more than 800 nM was required to reduce the binding to 50%. Almost no competition was observed for D'-D3 Glu787Ala. The data further reveal a biphasic competition curve for the Lys790Ala variant. This implies that D'-D3 Lys790Ala may exist in two conformations that differentially interfere with complex formation between FVIII and VWF. We

therefore cannot make any reliable conclusions about the putative role of Lys790 for FVIII binding. Based on the results, we also constructed two new D'-D3 variants *i.e.* Glu787Gln and Asp796Asn and assessed their FVIII binding efficiency using SPR analysis. Results showed that changing the charged amino acids with their neutral counterpart also affected FVIII binding (*Online Supplementary Figure S2*). Changing Glu787 for a Gln in full-length VWF also revealed a major impact on FVIII using a solid phase binding assay (*Online Supplementary Figure S3*). The data together confirm the observation that amino acid residues

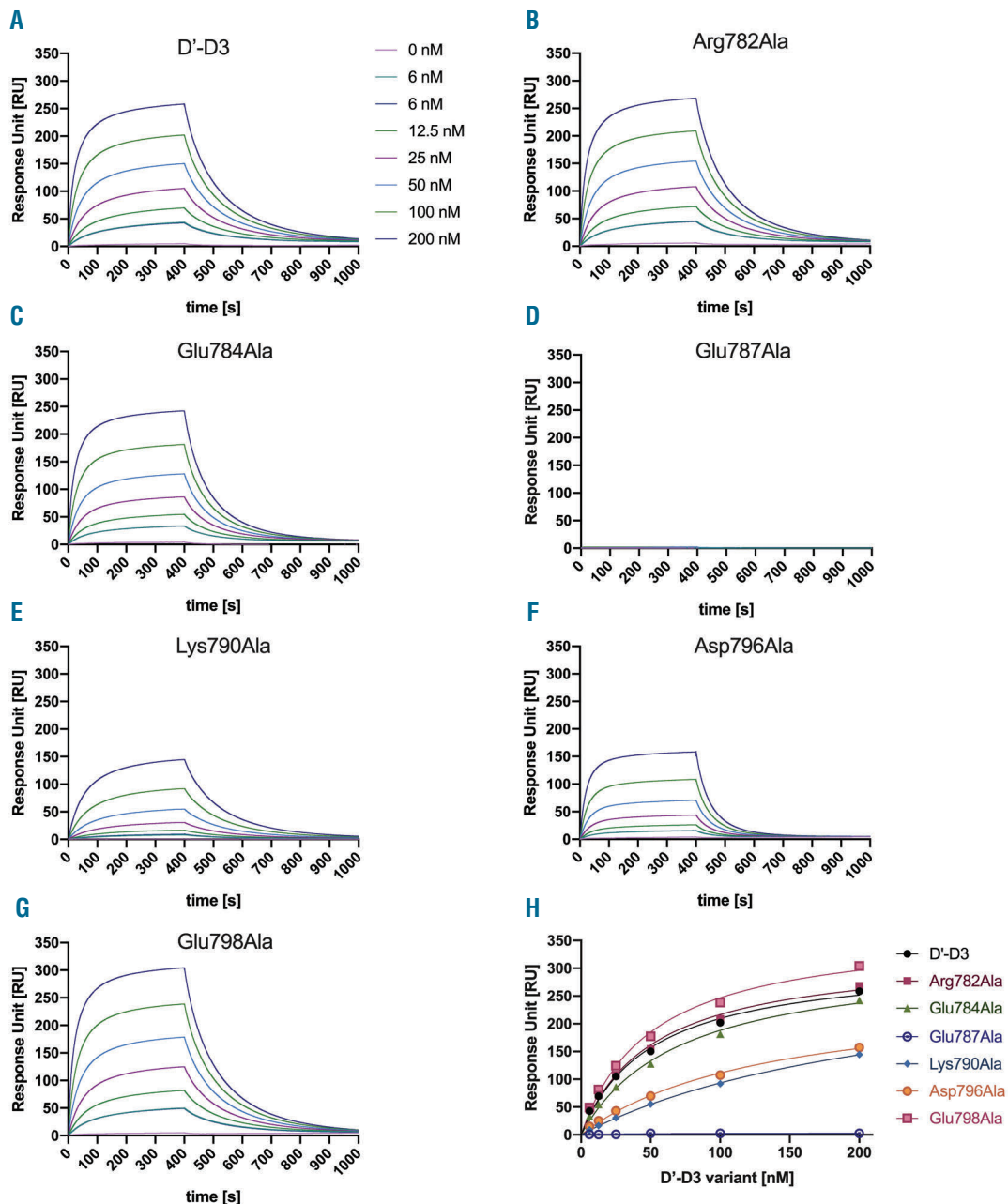


**Figure 3. Surface plasmon resonance analysis of D'-D3 variants in interaction with FVIII.** (A-G) Multiple concentrations (0-200 nM) of the indicated D'-D3 variants were passed over the coagulation factor VIII (FVIII) that was immobilized via antibody EL14 to the surface of a CM5 sensor chip. The binding response is represented in response units (RU) and was assessed in 20 mM HEPES (pH 7.4), 150 mM NaCl, 5 mM CaCl<sub>2</sub>, 0.05% (v/v) Tween 20 at a flow rate of 30  $\mu$ L/min at 25°C. (H) Shows the maximum binding response in RU of the D'-D3 variants at a function of the employed concentration.

in the region Arg782-Cys799 are involved in FVIII binding. In particular, the glutamic acid residue at position 787 seems critical for the interaction between FVIII and D'-D3.

### A leucine at position 786 is important for effective interaction with FVIII

Analysis of the crystal structure of D'-D3 shows that Glu787 is part of a short helical region that also includes Leu786 and Cys788 (Figure 5A).<sup>30</sup> We speculate Leu786 and Cys788 are critical to maintain the structural integrity of this helix, and therefore the spatial position of Glu787 in D'-D3. We therefore decided to destabilize this helical structure by replacing Leu786 for an alanine residue and study the effect thereof on FVIII binding. SPR analysis showed a markedly reduced FVIII binding response of the Leu786Ala variant with an estimated  $K_d$  of ~500 nM (Figure 5C). The competitive binding assay revealed that about 400 nM of the variant was required to reduce FVIII binding to VWF by 50% (Figure 5B). These findings together demonstrate an impaired FVIII binding efficiency of D'-D3 Leu786Ala. We propose therefore that the stability of the helical region may indeed be of importance for FVIII binding.

### Discussion

The particularly high complexity of the molecular architecture of VWF has always posed a major challenge for the identification of the FVIII interactive regions within VWF. We therefore decided to utilize a short fragment of VWF that includes the FVIII binding site, *i.e.* D'-D3.<sup>2</sup> Previously, we have employed a primary amine-directed chemical footprinting approach on the FVIII-VWF complex and established that Lys773 contributes to FVIII binding.<sup>23</sup> This approach provided only information about the putative

role of the side-chains of lysine amino acid residues for FVIII-VWF complex formation. HDX-MS as utilized in this study has the potential to provide information about the putative role of all amino acids in D'-D3.<sup>33</sup>

With HDX-MS, the replacement of amide hydrogen atoms of the protein backbone by deuterium atoms can be assessed upon the transfer of a protein complex from H<sub>2</sub>O to D<sub>2</sub>O. Sites where proteins interact can show a reduced time-dependent deuterium incorporation usually because of local changes in the hydrogen bonding network of the protein backbone. This methodology has proven to be particularly powerful in the identification of protein interaction sites.<sup>34</sup> Applying HDX-MS on the FVIII-D'-D3 complex showed reduced deuterium incorporation in amino acid region Arg782-Cys799 in the presence of FVIII (Figure 2). This result strongly suggest that it is involved in the interaction with FVIII. This region is also particularly rich in amino acid residues that are mutated in VWD type 2N (Figure 6). This corroborates the functional importance of this region.

The role of Arg782-Cys799 for FVIII binding was further confirmed by replacing the charged amino acid residues by alanine residues. Especially replacement of Glu787 proved detrimental for the interaction between D'-D3 and FVIII (Figures 3-4). A major impact on FVIII binding was also observed for the Glu787Gln variant of D'D3 and full-length VWF (*Online Supplementary Figure S2-3*). Patients with VWF type 2N have further been identified with a Glu787Lys variant of VWF.<sup>35</sup> These observations together demonstrate the importance of a glutamic acid at position 787. We cannot exclude that Glu787 may be critical for maintaining the local conformation of the D' domain. The crystal structure, however, reveals that Glu787 is exposed to the solvent and is not part of the internal protein core (Figure 5A).<sup>30</sup> We may therefore have identified one of the critical amino acids that directly

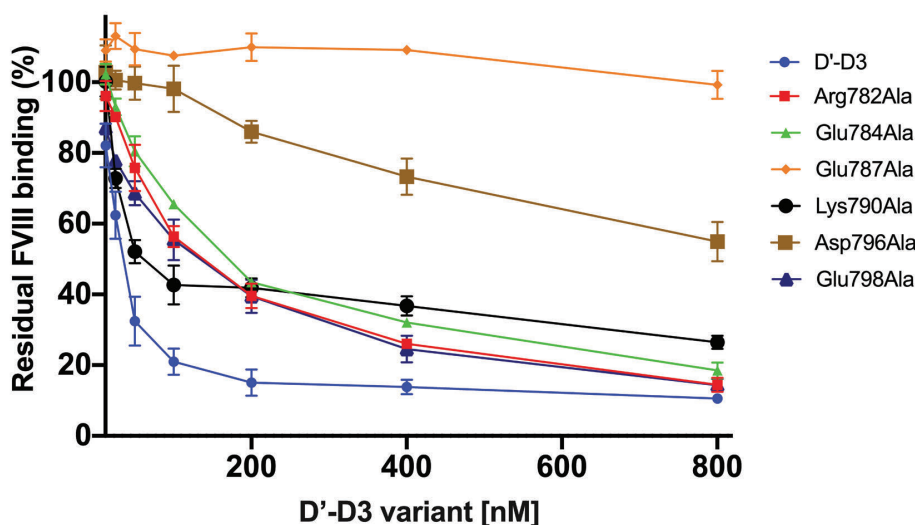


**Figure 4.** D'-D3 variants in competition with immobilized von Willebrand factor for binding FVIII. Coagulation factor VIII (FVIII) was incubated with increasing concentrations of the indicated D'-D3 variants in a buffer comprising 50 mM Tris (pH 7.4), 150 mM NaCl, 5mM CaCl<sub>2</sub>, 2% human serum albumin and 0.1% Tween 20 at 37 °C. The protein mixtures were next incubated with immobilized von Willebrand factor (VWF) in the same buffer. Residual FVIII binding to immobilized VWF was assessed employing HRP-conjugated CAg12 antibody as described in the methods. Data represents mean ± standard deviation (SD) of three independent experiments.

interacts with FVIII rather than being important for stabilizing the local conformation. The replacement of Leu786 by an alanine, most likely, alters the conformation of the short helical region 786-Leu-Glu-Cys-789 thereby repositioning Glu787 (Figure 5A). This can explain, in our view,

the altered FVIII binding efficiency of the Leu786Ala variant (Figure 5B-C). HDX-MS did not reveal reduced deuterium incorporation in peptides that include Lys773. This residue is part of a beta-sheet in which the amino backbone hydrogens tightly interact. Apparently, this second-

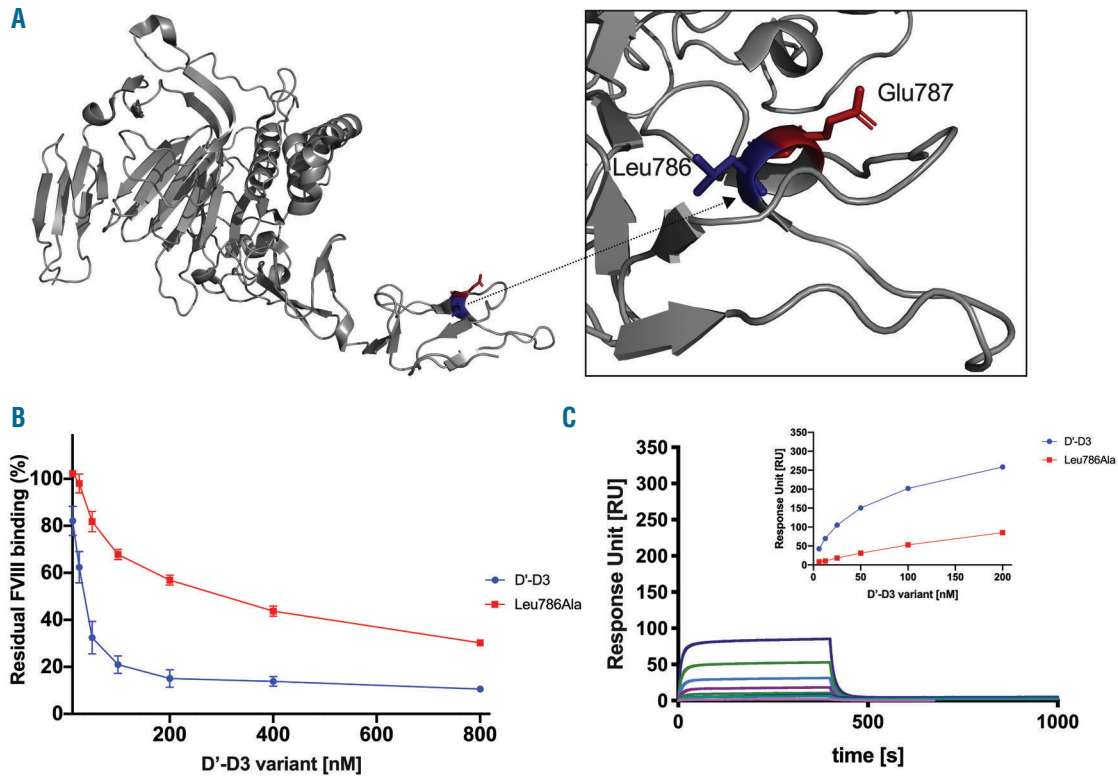


**Figure 5. The FVIII binding efficiency of D'-D3 Leu786Ala.** (A) Part of the crystal structure of D'-D3 (PDB entry: 6n29)30 with a zoom-in of the helical region comprising the residues 786-Leu-Glu-Cys-789. (B) Multiple concentrations of D'-D3 Leu786Ala were passed over coagulation factor VIII (FVIII) that was immobilized via antibody EL14 to the surface of a CM5 sensor chip. The binding response is indicated as response units (RU) and was assessed in 20 mM HEPES (pH 7.4), 150 mM NaCl, 5 mM CaCl<sub>2</sub>, 0.05% (v/v) Tween 20 at a flow rate of 30  $\mu$ L/min at 25°C. (C) FVIII was pre-incubated with increasing concentrations of D'-D3 and D'-D3 Leu786Ala in a buffer comprising 50 mM Tris (pH 7.4), 150 mM NaCl, 5mM CaCl<sub>2</sub>, 2% human serum albumin and 0.1% Tween 20 at 37 °C. The protein mixtures were next incubated with immobilized von Willebrand factor (VWF) in the same buffer. Residual FVIII binding to immobilized VWF was assessed employing HRP-conjugated CAg12 antibody as described in the methods. Data represents mean  $\pm$  standard deviation (SD) of three independent experiments.

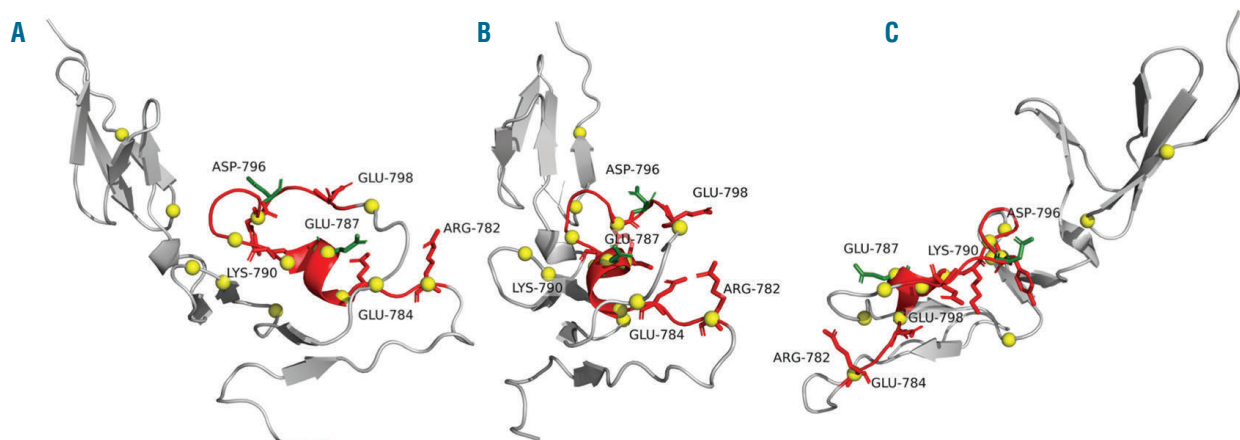


**Figure 6. Amino acid region Arg782-Cys799 and sites involved in von Willebrand disease type 2 Normandy indicated in the crystal structure of TIL' subdomain.** Shown is the TIL' subdomain of the crystal structure of the D'-D3 (PDB entry: 6n29) in a ribbon representation. (A-C) Present the same structure from different angles. Region Arg782-Cys799 is displayed in red. The yellow spheres indicated residues that have been mutated in the von Willebrand disease type 2 Normandy (VWD type 2N).<sup>37</sup>



ary structure element does not change its conformation upon FVIII binding, which is required to detect altered deuterium incorporation.

Based on cryo-EM studies, Yee *et al.* proposed a model for the FVIII-D'-D3 complex. In this model the D' domain is in contact with the FVIII C1 domain.<sup>18</sup> The contribution of the C1 domain to VWF binding has also been demonstrated with HDX-MS studies on FVIII in the presence and of the D'-D3.<sup>19</sup> Because of the relatively low resolution of the structure, it was not possible to predict the orientation of the D' domain on FVIII. Results of this study now provide evidence that the region comprising Arg782-Lys790 may be oriented towards the C1 domain of FVIII. This sequence is part of a flat surface on the TIL' subdomain that may optimally interact with the C1 domain (*Online Supplementary Figure S4*).

How the sulphated acid a3 region at the start of the FVIII A3 domain interacts with D'-D3 remains, however, unclear from both the cryo-EM study and this study. Removal of this region upon activation of FVIII is the trigger for FVIII-VWF complex dissociation.<sup>12</sup> It has further

been shown that replacement of the sulphated tyrosine residue 1680 with a phenylalanine leads to a VWF binding defect.<sup>14</sup> Recently, a well-designed nuclear magnetic resonance study was employed to assess the putative complex formation between the isolated a3 region and the isolated D' domain. Main changes in chemical shift were identified outside the region that was identified in our study, *i.e.* residues Val772, Asn819, Cys821 and Val 822, suggesting that the a3 region may interact with these residues. The isolated a3 binds the D' domain with a markedly reduced affinity compared to intact FVIII.<sup>36</sup> We have also found that the VWD3 subdomain of the D3 domain is required to support D' binding to FVIII as well.<sup>22</sup> These notions show that the mechanism by which FVIII and VWF interact and the role of the a3 region therein remains a topic for further investigation.

### Funding

*This study has been funded by Product and Process Development, Sanquin, the Netherlands (PPOP-13-002) and by the Landsteiner foundation of blood research (LSBR 1882).*

### References

- Brinkhous KM, Sandberg H, Garris JB, et al. Purified human factor VIII procoagulant protein: Comparative hemostatic response after infusions into hemophilic and von Willebrand disease dogs. *Proc Natl Acad Sci U S A*. 1985;82(24):8752-8756.
- Yee A, Gildersleeve RD, Gu S, et al. A von Willebrand factor fragment containing the D'D3 domains is sufficient to stabilize coagulation factor VIII in mice. *Blood*. 2014;124(3):445-452.
- Pipe SW, Montgomery RR, Pratt KP, Lenting PJ, Lillicrap D. Life in the shadow of a dominant partner: the FVIII-VWF association and its clinical implications for hemophilia A. *Blood*. 2016;128(16):2007-2016.
- Mazurier C, Goudemand J, Hilbert L, et al. Type 2N von Willebrand disease: clinical manifestations, pathophysiology, laboratory diagnosis and molecular biology. *Best Pract Res Clin Haematol*. 2001;14(2):337-347.
- Jorieux S, Fressinaud E, Goudemand J, et al. Conformational changes in the D' domain of von Willebrand factor induced by CYS 25 and CYS 95 mutations lead to factor VIII binding defect and multimeric impairment. *Blood*. 2000;95(10):3139-3145.
- Jorieux S, Gaucher C, Goudemand J, Mazurier C. A Novel mutation in the D3 domain of von Willebrand factor markedly decreases its ability to bind Factor VIII and affects its multimerization. *Blood*. 1998; 92(12):4663-4670.
- Springer TA. Biology and physics of von Willebrand factor concatamers. *J Thromb Haemost*. 2011;9 Suppl 1:130-143.
- Zhou YF, Eng ET, Zhu J, et al. Sequence and structure relationships within von Willebrand factor. *Blood*. 2012;120(2):449-458.
- Marti T, Rösselet SJ, Titani K, Walsh KA. Identification of disulfide-bridged substructures within human von Willebrand factor. *Biochemistry*. 1987;26(25):8099-8109.
- Fay P. Factor VIII Structure and function. *Int J Hematol*. 2006;83(2):103-108.
- Stoilova-McPhie S, Villoutreix BO, Mertens K, Kembell-Cook G, Holzenburg A. 3-Dimensional structure of membrane-bound coagulation factor VIII: Modeling of the factor VIII heterodimer within a 3-dimensional density map derived by electron crystallography. *Blood*. 2002;99(4):1215-1223.
- Lenting PJ, van Mourik JA, Mertens K. The life cycle of coagulation factor VIII in view of its structure and function. *Blood*. 1997;92(11):3983-3996.
- Saenko EL, Scandella D. The acidic region of the factor VIII light chain and the C2 domain together form the high affinity binding site for von willebrand factor. *J Biol Chem*. 1997;272(29):18007-18014.
- Leyte A, van Schijndel HB, Niehrs C, et al. Sulfation of Tyr 1680 of human blood coagulation factor VIII is essential for the interaction of factor VIII with von Willebrand factor. *J Biol Chem*. 1991;266(2):740-746.
- Hamer R, Koedam J, Besser-visser N, et al. Factor VIII binds to von Willebrand factor via its 80,000 light chain. *Eur J Biochem*. 1987;166(1):37-43.
- Leyte A, Verbeet MP, Brodniewicz-Proba T, Van Mourik JA, Mertens K. The interaction between human blood-coagulation factor VIII and von Willebrand factor. Characterization of a high-affinity binding site on factor VIII. *Biochem J*. 1989;257(3):679-683.
- Lollar P, Hill-Eubanks DC, Parker CG. Association of the factor VIII light chain with von Willebrand factor. *J Biol Chem*. 1988;263(21):10451-10455.
- Yee A, Oleskie AN, Dosey AM, et al. Visualization of an N-terminal fragment of von Willebrand factor in complex with factor VIII. *Blood*. 2015;126(8):939-943.
- Chiu P-L, Bou-Assaf GM, Chhabra ES, et al. Mapping the interaction between factor VIII and von Willebrand factor by electron microscopy and mass spectrometry. *Blood*. 2015;126(8):935-938.
- Fay PJ. Activation of factor VIII and mechanisms of cofactor action. *Blood Rev*. 2004;18(1):1-15.
- Foster PA, Fulcher CA, Marti T, Titani K, Zimmerman TS. A major factor VIII binding domain resides within the amino-terminal 272 amino acid residues of von Willebrand factor. *J Biol Chem*. 1987;262(18):8443-8446.
- Przeradzka MA, Meems H, van der Zwaan C, et al. The D' domain of von Willebrand factor requires the presence of the D3 domain for optimal factor VIII binding. *Biochem J*. 2018;475(17):2819-2830.
- Castro-Núñez L, Bloem E, Boon-Spijker MG, et al. Distinct roles of Ser-764 and Lys-773 at the N terminus of von Willebrand factor in complex assembly with coagulation factor VIII. *J Biol Chem*. 2013;288(1):393-400.
- van den Biggelaar M, Meijer AB, Voorberg J, Mertens K. Intracellular cotrafficking of factor VIII and von Willebrand factor type 2N variants to storage organelles. *Blood*. 2009;113(13):3102-3109.
- Stel HV, Sakariassen KS, Scholte BJ, et al. Characterization of 25 Monoclonal antibodies to FVIII-von Willebrand factor: relationship between ristocetin-induced platelet aggregation and platelet adherence to subendothelium. *Blood*. 1984;63(6):1408-1415.
- Meems H, Van Den Biggelaar M, Rondaij M, et al. C1 domain residues Lys 2092 and Phe 2093 are of major importance for the endocytic uptake of coagulation factor VIII. *Int J Biochem Cell Biol*. 2011;43(8):1114-1121.
- Bloem E, Meems H, van den Biggelaar M, et al. Mass spectrometry-assisted study reveals that lysine residues 1967 and 1968 have opposite contribution to stability of activated factor VIII. *J Biol Chem*. 2012;287(8):5775-5783.
- van den Biggelaar M, Bouwens EAM, Voorberg J, Mertens K. Storage of factor VIII variants with impaired von Willebrand



- factor binding in Weibel-Palade bodies in endothelial cells. *PLoS One*. 2011;6(8):e24163.
29. Purvis AR, Gross J, Dang LT, et al. Two Cys residues essential for von Willebrand factor multimer assembly in the Golgi. *Proc Natl Acad Sci U S A*. 2007;104(40):15647-15652.
  30. Dong X, Leksa NC, Chhabra ES, et al. The von Willebrand factor D'D3 assembly and structural principles for factor VIII binding and concatemer biogenesis. *Blood*. 2019;133(14):1523-1533.
  31. Dimitrov JD, Christophe OD, Kang J, et al. Thermodynamic analysis of the interaction of factor VIII with von Willebrand factor. *Biochemistry*. 2012;51(20):4108-4116.
  32. Owen WG, Wagner RH. Antihemophilic factor: separation of an active fragment following dissociation by salts or detergents. *Thromb Diath Haemorrh*. 1972;27(3):502-515.
  33. Marcsisin SR, Engen JR. Hydrogen exchange mass spectrometry: what is it and what can it tell us? *Anal Bioanal Chem*. 2010;397(3):967-972.
  34. Morgan CR, Engen JR. Investigating solution-phase protein structure and dynamics by hydrogen exchange mass spectrometry. *Curr Protoc Protein Sci*. 2009;Chapter 17:Unit 17.6.1-17.
  35. Schneppenheim R, Budde U, Drewke E, et al. Results of a screening for von Willebrand disease type 2N in patients with suspected haemophilia A or von Willebrand disease type 1. *Thromb Haemost*. 1996;76(4):598-602.
  36. Dagil L, Troelsen KS, Bolt G, et al. Interaction Between the  $\alpha 3$  Region of Factor VIII and the TIL'E' Domains of the von Willebrand Factor. *Biophys. J*. 2019;117(3):479-489.
  37. de Jong A, Eikenboom J. Von Willebrand disease mutation spectrum and associated mutation mechanisms. *Thromb Res*. 2017;159:65-75.